World Scientific
www.worldscientific.com

DESIGN OF ASSISTIVE WHEELCHAIR SYSTEM DIRECTLY STEERED BY HUMAN THOUGHTS

JUNHUA LI* and JIANYI LIANG

MOE-Microsoft Key Laboratory for Intelligent Computing and Intelligent Systems
Department of Computer Science and Engineering
Shanghai Jiao Tong University, Shanghai 200240, P. R. China
*juhalee@sjtu.edu.cn

QIBIN ZHAO

Laboratory for Advanced Brain Signal Processing
Brain Science Institute, RIKEN
Wako-shi, Saitama 351-0198, Japan

JIE LI

Department of Computer Science and Technology
Tong Ji University, Shanghai 200092, P. R. China

KAN HONG and LIQING ZHANG[†]

MOE-Microsoft Key Laboratory for Intelligent Computing and Intelligent Systems
Department of Computer Science and Engineering
Shanghai Jiao Tong University, Shanghai 200240, P. R. China
†zhang-lq@cs.sjtu.edu.cn

Integration of brain–computer interface (BCI) technique and assistive device is one of chief and promising applications of BCI system. With BCI technique, people with disabilities do not have to communicate with external environment through traditional and natural pathways like peripheral nerves and muscles, and could achieve it only by their brain activities. In this paper, we designed an electroencephalogram (EEG)-based wheelchair which can be steered by users' own thoughts without any other involvements. We evaluated the feasibility of BCI-based wheelchair in terms of accuracies and real-world testing. The results demonstrate that our BCI wheelchair is of good performance not only in accuracy, but also in practical running testing in a real environment. This fact implies that people can steer wheelchair only by their thoughts, and may have a potential perspective in daily application for disabled people.

Keywords: Assistive wheelchair; brain–computer interface; EEG; motor imagery.

1. Introduction

With the change of population structure in the world, the proportion of elder people is increasing quickly, especially in recent years. One challenge accompanying the change of population structure is that the number of disabled people is also dramatically increasing. This leads to an increase for requirement of assistive devices, which are used to help people with disabilities restore lost functions. A wheelchair is the foremost assistive device for helping people who have an impediment in motor functionality. Researchers have developed wheelchair systems controlled by body part movements,[1,2] head or eyeball positions,[3] without the need for a joystick. However, these control methods are not applicable to be used by people with complete loss of motor

functionality due to the requirement of movements of body parts. Fortunately, brains of these people are largely unaffected and can generate different mental states. These different mental states could be detected through EEG, which can be adopted as a control signal to drive an external device (such as wheelchair, robot). So, those people can send a command to order device operation by modulation of mental state.

EEG is a common physiological signal to observe dynamics of human brain.[4] Due to its good properties, it has been utilized to investigate a variety of diseases such as Alzheimer's disease,[5–10] epilepsy,[11–16] autism.[17,18] For instance, wavelet-chaos methodology is used for automated diagnosis of epilepsy or Alzheimer's disease based on EEG signal.[19] Because EEG conveys real-time information reflecting brain status, some diseases can be diagnosed or some mental tasks can be detected by decoding EEG signals. Researchers have proposed a number of methods for decoding EEG signals.[20–25] These methods include preprocessing techniques for improving signal-to-noise ratio (SNR), feature extraction for capturing essential information, and classification methods for giving a judgment. Judgment from EEG decoding is then translated into commands to control an external device. Connecting directly between the human brain and an external device is known as a brain–computer interface (BCI).[26–29] Using a BCI, paralyzed patients can communicate with outside environment and operate external devices to overcome some limitations of paralyzed limbs or body parts. Up to now, several BCI systems have been successfully developed suitable for different applications such as two-dimensional (2D) or three-dimensional (3D) cursor control,[30–32] P300 word spelling system[33] and neuroprosthesis control.[34] Dandan Huang *et al.* has realized a virtual wheelchair,[35] which moves in a 2D plane displayed on a screen by event-related desynchronization/synchronization (ERD/ERS)[36] of EEG. In addition, researchers at Graz University of Technology proposed asynchronous BCI control of a wheelchair going through a virtual street.[37] And Galan *et al.* developed a wheelchair based on different kinds of mental tasks and evaluated it in a virtual environment.[38] For application in the real world, a P300-based wheelchair was designed to run on the predefined paths inside a typical office.[39,40] These

wheelchair systems either existed in the virtual environment or required predefined running paths. This restricts practical application in daily living. Hence, we built a brain-controlled wheelchair steered by ongoing EEG reflecting user's thoughts. It can be run in the real world and can be steered to go wherever user wants to reach.

For the rest of paper, we first introduce experimental setting including participants and EEG recording parameters. Then, system structure of assistive wheelchair and computational algorithm were detailed, and neural mechanism underlying specific mental tasks was interpreted. Subsequently, the evaluations of assistive wheelchair system were presented. After that, we compared our designed wheelchair system with the existed wheelchair systems in the section of discussion. At last, a conclusion was drawn to briefly summarize our work in this paper and to give a potential perspective about application of the brain-driven wheelchair system.

2. Materials and Methods

2.1. *Participants and recording instrument*

Three healthy participants attended evaluation of wheelchair. Their ages were in the range from 22 to 24 with mean of 23. All are right handed, and do not have any neurological or psychiatric disease. They all gave their informed consent forms for attending wheelchair evaluation after introduction of each step they should be engaged in the evaluation. Here, G.tec amplifier (Guger Technologies, Austria) was employed to continuously record EEG signals from the scalp and transfer these signals to a laptop. We set the sampling rate as $256\,\text{Hz}$ and kept each electrode below impedance of $5\,\text{k}\Omega$. During the recording period, participants were requested to keep motionless as well as possible. A total of 14 electrodes (i.e. C5, C3, C1, CZ, C2, C4, C6, CP5, CP3, CP1, CPZ, CP2, CP4 and CP6) over sensorimotor cortex were used for EEG recording. A ground electrode was located on medial frontal cortex. The averaged potential of two electrodes on bilateral earlobes was reference potential for EEG recording. All electrodes were mounted in a standard EEG cap according to the 10–20 international system criterion. Figure 1 illustrates all electrodes and their positions on the scalp.
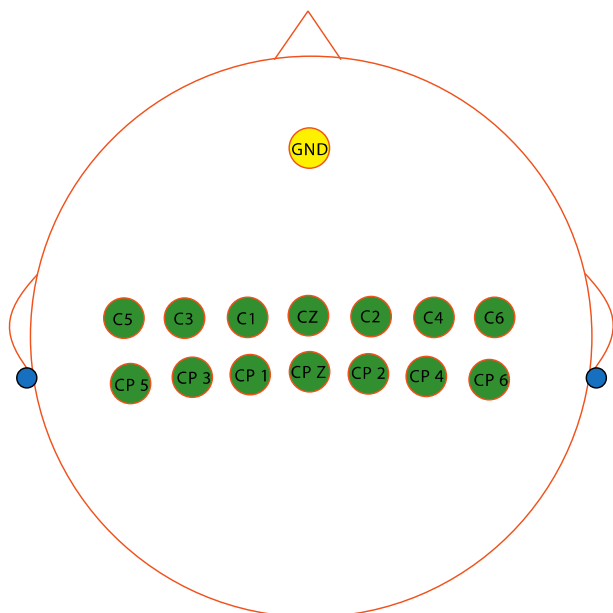
Fig. 1. (Color online) Electrodes distribution used for EEG recording in the brain-driven assistive wheelchair system. Green electrodes records EEG used for user's thoughts recognition. Blue electrodes located on bilateral earlobes are reference electrodes and yellow electrode serves as ground electrode.

Fig. 2. Wheelchair assistive system structure. BCI system is shown in black rectangle and wheelchair hardware system is enclosed in dashed box.

2.2. *System structure*

Our designed wheelchair system composes of two parts: BCI system and wheelchair hardware system. For a new user, models in BCI system should be trained before steering wheelchair online. By model training, all parameters in common spatial pattern (CSP)[41,42] and support vector machine (SVM)[43] are optimized to best separate three different mental tasks. Trained models subsequently serve to process real-time EEG signals. As shown in the black rectangle of Fig. 2, raw EEG is firstly preprocessed to improve the SNR. The preprocessing procedure includes two steps: threshold-based noise rejection and common average reference (CAR).[44] Threshold-based noise rejection removes segments, which are affected by extreme noise contamination (e.g. EMG). The value of rejection threshold can be chosen from pop-down menu on the GUI according to current user. Each channel is re-referenced to the averaged value of all channels through CAR to improve SNR. And then, the most discriminative features for current EEG segment are extracted by CSP trained based on preceding recorded EEG

data. Next, a SVM classifier is applied to recognize the user's current mental task (i.e. left hand motor imagery, right hand motor imagery and feet motor imagery).[45] Finally, the outputs of SVM classifier are optimized to obtain a wheelchair control command. According to this procedure, the BCI system translates users' thoughts into control commands.

The details about the processing from a preprocessed segment of EEG to classification are illustrated in the Fig. 3. Three CSP feature extractors are employed in a manner of one versus the rest. Namely, other two classes are treated as the same class when one class is chosen. So the problem of three-class is transformed to three two-class problems. For each two-class problem, features are extracted according to the following computation.

A segment of EEG signal is represented as an N by T matrix E, where N is the number of recording electrodes and T is the number of sampling points per electrode in a segment. The spatial covariance of a segment can be obtained from

$$C = E^* E', \tag{1}$$
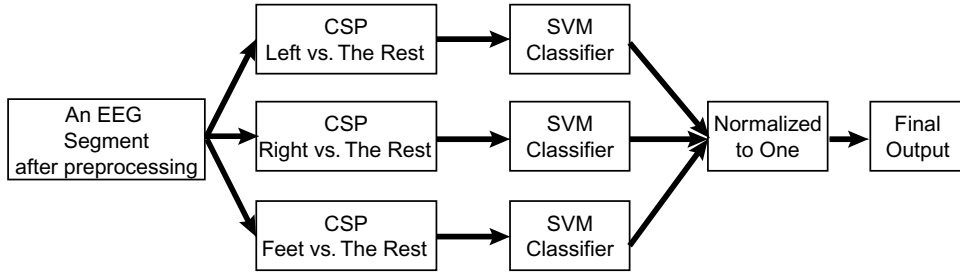
Fig. 3. The flowchart of feature extraction and classification for an EEG segment.

then C is normalized by following equation

$$C_n = \frac{C}{\text{trace}(C)}. \tag{2}$$

The EEG signals are separated into two groups according to the manner of one versus the rest (e.g. left motor imagery versus the rest classes: right motor imagery and feet motor imagery). Spatial covariance of each group is calculated, respectively by averaging over all segments of each group.

$$\bar{C}_{nw} = \frac{1}{n_w} \sum_{i=1}^{n_w} C_{nw} \quad w \in [x, \text{rest}], \tag{3}$$

where n_w is the number of segments corresponding to each group, w denotes which group it belongs to (x represents the chosen class, rest represents the rest classes). The sum spatial covariance is then given as

$$C_{nz} = \bar{C}_{nx} + \bar{C}_{n\,\text{rest}}. \tag{4}$$

C_{nz} is factored into the product of three matrices as

$$C_{nz} = U_z \lambda_z U_z', \tag{5}$$

where U_z is the matrix composed of eigenvectors and λ_z is the diagonal matrix of eigenvalues. We can obtain the whitening transformation matrix P by using

$$P = \sqrt{\frac{1}{\lambda_z}} U_z'. \tag{6}$$

If $\bar{C}_{nx}$ and $\bar{C}_{n\,\text{rest}}$ are individually transformed as

$$S_x = P \bar{C}_{nx} P'$$

and

$$S_{\text{rest}} = P \bar{C}_{n\,\text{rest}} P', \tag{7}$$

then S_x and S_{rest} share common principal components (common eigenvectors).[46] The sum of corresponding eigenvalues for the two matrices will always

be equal to one. That is, if S_x is factored as

$$S_x = F \lambda_x F'$$

and

$$S_{\text{rest}} = F \lambda_{\text{rest}} F', \tag{8}$$

then,

$$\lambda_x + \lambda_{\text{rest}} = I. \tag{9}$$

F spans a new space. From Eq. (9), we can see that the m eigenvectors corresponding to the m largest eigenvalues in λ_x will be maximal for EEG of the chosen class of motor imagery and minimal for EEG of the rest classes of motor imagery at the same time. Similarly, the reverse is true. The eigenvectors corresponding to the m largest and smallest eigenvalues, respectively are chosen because those eigenvectors contain maximal variance and are very useful for classification of EEG.

A segment of EEG is projected into space of common special patterns as orthogonal components by the projection matrix $V = F'P$. So a segment of EEG is projected formulating as

$$Z = VE. \tag{10}$$

We obtain $2m$ time series if m largest eigenvectors of each group are chosen. Then the $2m$ features are calculated for a segment (EEG data) by the following equation:

$$\text{feature}_i = \sum_{t=1}^{T} (z_i(t))^2 \quad i = 1, 2, \ldots, 2m, \tag{11}$$

where z_i represents row of Z and t is sampling time of a segment. In order to normalize the distribution of elements, features are reevaluated by the following

equation:

$$\text{feature}_i = \log\left(\frac{\text{feature}_i}{\sum_{j=1}^{2m} \text{feature}_j}\right). \quad (12)$$

According to this principle, three extractors, respectively assigned to each class of motor imagery, were generated and then those extracted features were respectively used for training corresponding SVM classifier. The SVM decision function is as follows:

$$f(X) = \text{sign}(\langle W, \phi(X)\rangle - b). \quad (13)$$

And, the maximal margin hyper-plane is

$$W = \sum_{i=1}^{m} \alpha_i y^i \phi(X^i), \quad (14)$$

where parameters α_i are positive real numbers when maximizing

$$\sum_{i=1}^{m} \alpha_i - \sum_{i,j=1}^{m} \alpha_i \alpha_j y^i y^j \langle \phi(X^i), \phi(X^j)\rangle \quad (15)$$

subject to

$$\sum_{i=1}^{m} \alpha_i y^i = 0, \quad \alpha_i > 0, \quad (16)$$

So, the SVM decision function can be reformulated as

$$f(X) = \text{sign}\left(\sum_{i=1}^{m} \alpha_i y^i \langle \phi(X^i), \phi(X)\rangle - b\right). \quad (17)$$

At the real-time classification phase, an EEG segment (1 s width, updated every 125 ms) was extracted to obtain features by three CSP extractors. Subsequently, the SVM classifier was respectively used to recognize features deriving from corresponding CSP extractor. Three SVM classifiers output probabilities for each class of motor imagery. In order to let the sum of probabilities of all classes be as one, we normalized outputted probabilities and got the final classification label for which there was the highest probability. After that, classification label was translated into a control command. The command was sent to wheelchair hardware system to control wheelchair movements.

The description of the wheelchair hardware system is mainly focused on hardware components assembled to execute commands of movements. As shown in the dashed box of Fig. 2, the commands are firstly converted into analog signal using a digital to analog convertor. Then, after transferring the analog signal to the control board, the control board drives two electric motors that provide power to steer wheelchair. Two analog signals are, respectively used to accomplish wheelchair actions of turning and going forward. The wheelchair keeps motionless when two analog signals are set to be the voltage of 2.5. Decreasing of voltage for turning analog signal will make wheelchair turn left. On the contrary, increasing of voltage makes wheelchair turn right. The more bias from balanced voltage (2.5) control voltage is, the faster the speed. The other analog signal is used for the control of going forward, and voltage increasing of that analog signal speeds up the wheelchair to go forward. The electrical power of electric motors is provided by lead-acid battery, which is located under the seat of wheelchair. The battery with a full charge can provide power to drive wheelchair 20 km approximately. There is a safety switch among convertor, joystick and control board. This switch is used to switch control ways between EEG-based control and joystick-based control. It also provides a function of emergency brake through transferring safety switch when it is necessary. It should be noted that safety switch is useful for conditions of new user with a bad control performance or an emergency encountered. By real-time EEG classification and command execution, users would adjust their brain activities to make wheelchair reach where they expect and to achieve movement independently.

In order to improve performance of wheelchair and facilitate user's operation, we set optimization rules to optimize control commands. Optimization rules include:

- Starting Optimization: A more powerful force output from electric motor is needed when wheelchair is changing from stationary state to motion state due to the effect of inertia. So we set a higher voltage for that case. For example, an extra 20% volume of predefined voltage (which can be set on the GUI) is added to let electric motors output a stronger power, and then the voltage is slowly decreased to the predefined voltage.
- Operation Smoothness Optimization: This is mainly through ignoring peculiar commands (like a right turning command is ignored if it appears in a sequence of forward commands) to make wheelchair run smoothly.

- Speed Optimization: This aims to shorten running time when a long distance with the same direction is needed to go, which is accomplished through giving an acceleration when several consecutive commands belong to the same class. Acceleration is activated when several continuously similar commands are received. So it is judged based on recognition results of the specified recent period.
- Turning Optimization: This is used to solve the problem that rear-wheels are hard to position when direction of wheelchair is changed. For example, a strong and sustained turning command will be given when a few commands (those commands do not have to be required continuous outputs. That is other direction commands are allowed to be among those commands, but not too many) for same direction turning are detected.

All above optimization strategies are embedded into the program. The flow of optimization algorithm program is listed as follows.

Optimization Strategies Algorithm

---

1 While 1
2   If stopping signal = false
3   If a new output is coming
4   checking class labels of current and several previous outputs
5   Switch
6   Case1:previous nearest output is empty
7   giving a more powerful force
8   Case2:current class = previous class
9   the number of that class increases by 1
10   If accumulative number >= threshold
11   giving an acceleration
12   EndIf
13   Case3:current output is peculiar
14   ignoring current output
15   Case4:current output is turning command
16   turning optimization
17   Otherwise
18   giving a normal output
19   EndSwitch
20   EndIf
21   Else
22   break out of loop
23   EndIf
24 EndWhile

2.3. Neural mechanism

We adopted EEG measured from sensorimotor cortex as control signal to steer wheelchair without any other involvements. Three mental tasks, respectively make wheelchair turn left, turn right and go forward (left and right motor imageries to turn left and turn right, respectively, feet motor imagery to go forward). The principle is based on that the spectral representation of EEG is different when a user imagines different types of mental tasks. Figure 4 shows three typical channels, respectively located on left and right hemispheres and a central area. The three rows at the top of Fig. 4 show averaged time-frequency decompositions across all trials corresponding to left motor imagery, right motor imagery and feet motor imagery, respectively. From the first row, we can clearly see that spectral power from 5 to 15 Hz on left hemisphere (C3 is located on left hemisphere) is higher than that of right hemisphere (C4 is on right hemisphere) when the user is imagining left hand movements. In contrast, spectral power of left hemisphere is lower than that of right hemisphere when the user is imagining right hand movements (see the second row of Fig. 4). This shows an obvious contralateral power augmentation relevant to motor imageries. Under feet motor imagery, the spectral power in bilateral hemispheres is higher than the spectral power in central area (see the third row of Fig. 4). The lowest row in Fig. 4 depicted density of spectral power at frequencies from 2 to 50 Hz. Blue, red and black lines in each plot correspond to left, right and feet motor imageries, respectively (plots from left to right correspond to channels C3, CZ, C4, respectively). Density of spectral power of left motor imagery is greater compared with right motor imagery at channel C3. A reverse phenomenon is found at channel C4. Taking three plots together, we can see that PSD of feet motor imagery is greater than that of other two motor imageries at each channel, and lower density is shown at channel CZ. Hence, the BCI system recognizes user's movement intentions according to changes in spectral power relevant to user's mental tasks.

2.4. Graphical user interface (GUI)

A GUI (see Fig. 5) is provided by assistive wheelchair system so as to allow caregivers to expediently customize system configuration. This is useful due to
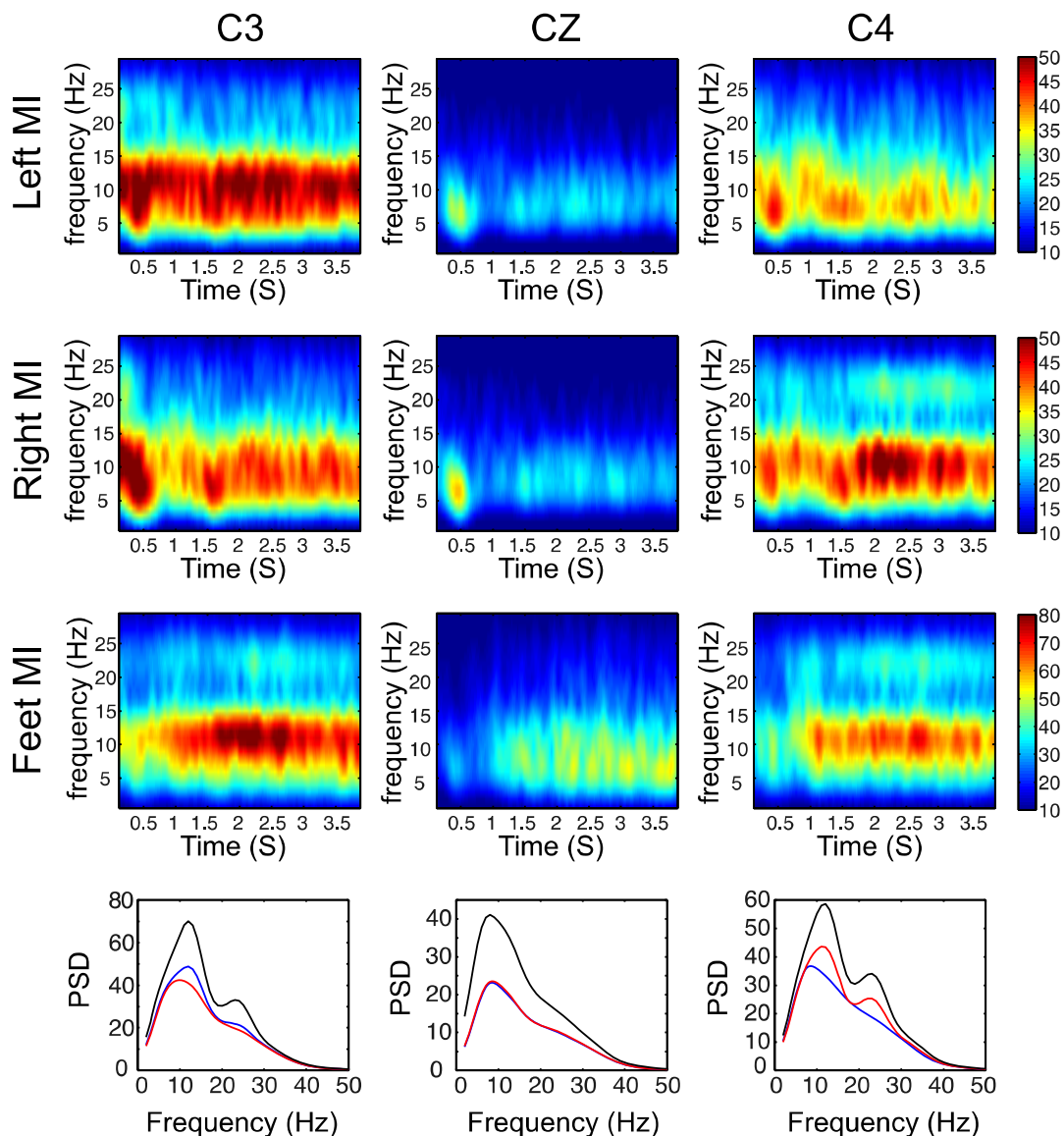
Fig. 4.   (Color online) Spectral representations in different motor imageries (i.e. left motor imagery, right motor imagery and feet motor imagery. MI stands for motor imagery.) The top three rows are time-frequency decomposition for motor imageries at typical electrode sites. The last row at the bottom shows power spectral density (PSD). Blue, red and black lines, respectively correspond to left, right and feet motor imageries.

that different users have different operation preferences. A configuration suitable for current user will facilitate wheelchair control, and achieve an expected performance. For example, a user with a poor performance of specific class of motor imagery needs a lower threshold for that class of motor imagery to make corresponding control command generate more easily than that of the other two classes of motor imagery. Besides some options, such as voting

method, sliding window width, step length, are also provided on the GUI to construct BCI system with high performance. The more options the GUI provides to set, the more easily a specialized BCI system with good performance could be built. But the problem is concomitantly appeared. Those who are not familiar with this system configuration are not recommended to configure advanced options (e.g. voting method, width of sliding time window). We advise
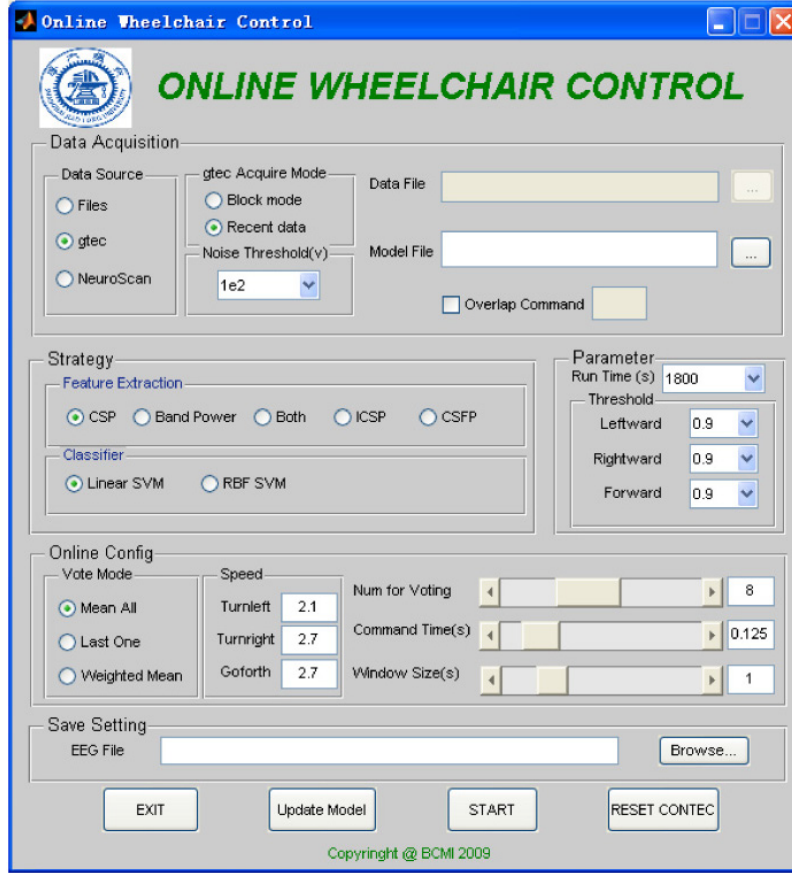
Fig. 5.   The GUI for assistive wheelchair control system.

them to use default configuration with only modification of thresholds for outputting commands of each class.

3.   Results

We evaluated the EEG-based wheelchair system in terms of accuracies and practical running testing in a real environment. At accuracy evaluation, we checked trial and sliding time window accuracies for each participant. There were four sessions conducted by each participant for evaluation. A session comprised 12 trials. Every trial was four-second length and was divided into 25 sliding time windows by that a window with width of 1 s slid forward every 125 ms. Each sliding time window as a segment of EEG was classified, and then sliding time window accuracy was obtained by counting the number of correct classifications as follows:

$$\text{ACC}_\text{STW} = \frac{N_\text{correct}}{N_\text{total}}. \qquad (18)$$

Trial probabilities assigned to each class of motor imagery were calculated by averaging all probability outputs of sliding time windows within that trial

$$\text{PRO}_T = \frac{1}{25} \sum_{i=1}^{25} \text{PRO}_{\text{STW}(i)}$$

$$= \frac{1}{25} \sum_{i=1}^{25} \begin{pmatrix} \text{pro}^1_\text{STW}(i) \\ \text{pro}^2_\text{STW}(i) \\ \text{pro}^3_\text{STW}(i) \end{pmatrix}, \qquad (19)$$

where PRO_T is a vector with three rows, and each row is the probability corresponding to each class of motor imagery. pro^1_STW, pro^2_STW and pro^3_STW are, respectively probabilities of sliding time window of left, right and feet motor imageries. Accordingly, trial accuracy was obtained by counting the number of trials classified correctly

$$\text{ACC}_T = \frac{N_\text{correct}}{N_\text{total}}. \qquad (20)$$

Table 1. The accuracies under conditions of trial and sliding time window for each participant and averaged accuracies.

Participant	Trial accuracy (%)	Sliding time window accuracy (%)
1	75.67	64.54
2	83.00	69.11
3	89.00	76.11
Mean	82.56	69.92

The accuracy results are listed in the Table 1. All participants achieved a performance much higher than chance level (33.33%). Averaged accuracy of sliding time window was 69.92% and averaged trial accuracy was increased to 82.56%. Trial accuracies were generally higher than accuracies of sliding time window because trial accuracy was calculated by averaging all sliding time windows within that trial.

Participant 2 further attended a practical driving testing, in which we evaluated practical performance when wheelchair is running in an environment with
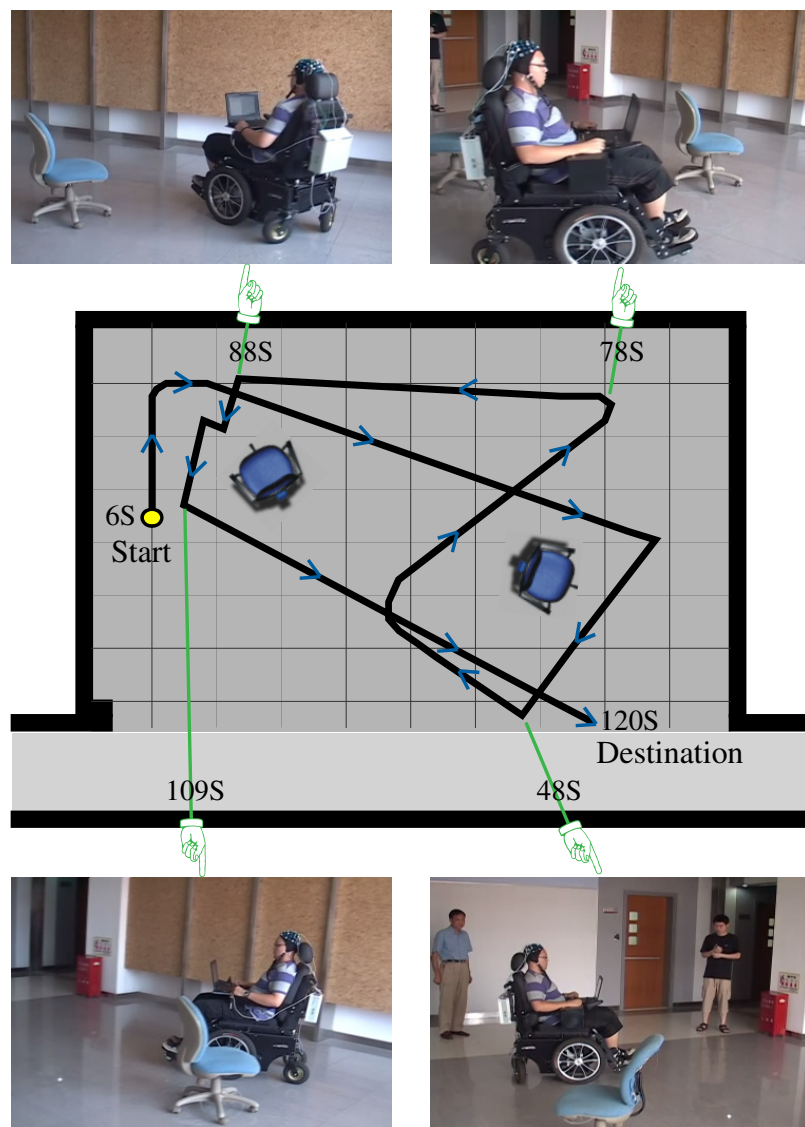
Fig. 6. Practical driving testing of EEG-based wheelchair assistive system. The central panel shows trajectory of wheelchair passed. Four snapshots around central panel are scenes at specified time points.

obstacles (see Fig. 6). The participant was required to steer the wheelchair moving along a specific path without hitting the obstacles (that are chairs). The testing demonstrated that the wheelchair can be directly controlled by EEG and can be steered according to user's intentions. A good performance, such as smooth movement and obstacle avoidance, was observed. As shown in Fig. 6, central drawing exhibits the trajectory of wheelchair passed, and surrounding four snapshots show scenes at specific points in time. The entire video about practical wheelchair testing in a real environment can be found at http://bcmi.sjtu.edu.cn/eegwheelchair.html.

4. Discussions

Our designed wheelchair was of favorable properties compared with other existed wheelchair systems. In the wheelchair system, thoughts were adopted as command to steer movements of wheelchair, rather than controlled by movements of body part (such as lips' movements) as described in Refs. 1 and 2. Thought-based controlling does not require any movement of any body part and thus can be used by a paralyzed patient. The wheelchair developed by Galan *et al.* was based on thoughts, but three different kinds of mental tasks were used to accomplish three direction movements (left hand imagination to turn left, rest to go forward and words association to turn right).[38] The mapping between mental task and wheelchair movement is not very intuitive to a user and might confuse them in some cases. A more natural and accustomed mapping (left and right motor imageries to turn left and turn right respectively, feet motor imagery to go forward) was employed in our designed wheelchair. It could reduce mental load without remembering mapping relationship, and could make the user only focus on motor imagery to improve performance. Additionally, we evaluated our wheelchair system in a real world, rather than a simulated virtual world as described in Galan's literature.[38] Compared with Rebsamen *et al.*'s paper,[39] our BCI paradigm is different from their P300 paradigm. Before using their wheelchair, paths need to be predefined. And, only presetting destinations can be reached. However, our wheelchair can be steered to wherever the user wants to go. Modification of paths is troublesome and time consuming in their wheelchair system, but it must

be done once assignment of environment has been changed. Particularly, in the case of that a user lives with a pet, it would cause extra trouble that pet could block the predefined path.

For the future, two aspects might be considered to further improve the usability of our assistive wheelchair system. First, we could integrate infrared sensors into the wheelchair system. The infrared sensors are used to measure distance between wheelchair and obstacles. If the distance between them is less than a specific value (e.g. 20 cm), wheelchair will stop whatever given command is. This ensures that wheelchair does not hit obstacles, even when user gives a wrong command under some situations. The other is that we could adopt other types of EEG signal. For example, steady state visual evoked potential (SSVEP) could be utilized as a supplementary control signal to improve control performance of wheelchair. Sometimes, heart rate could even be adopted as a reference signal. Because heart rate is dramatically increased when user encounters an emergency.

5. Conclusions

We designed an EEG-based wheelchair system which is directly steered by users' thoughts. The results of accuracies and practical testing showed that the wheelchair achieved a good performance and can be controlled to move smoothly in an environment with obstacles. This suggests that our designed wheelchair system might have a potential perspective for applying it to people with disabilities in daily life, which would strengthen independence of their daily living and make them feel happier.

References

1. J. S. Ju, Y. Shin and E. Y. Kim, Intelligent wheelchair using head tilt and mouth shape, *Electron Lett.* **45**(17) (2009) 873–875.
2. C. S. L. Tsui, P. Jia, J. Q. Gan, H. Hu and K. Yuan, EMG-based hands-free wheelchair control with EOG

attention shift detection, *IEEE International Conf. Robotics and Biomimetics* (Sanya, China, 2007), pp. 1266–1271.

3. Q. X. Nguyen and S. Jo, Electric wheelchair control using head pose free eye-gaze tracker, *Electron Lett.* **48**(13) (2012) 750–752.

4. M. Ahmadlou and H. Adeli, Functional community analysis of brain: A new approach for EEG-based investigation of the brain pathology, *NeuroImage* **58**(2) (2011) 401–408.

5. M. Ahmadlou, H. Adeli and A. Adeli, New diagnostic EEG markers of the Alzheimer's disease using visibility graph, *J. Neural Transm.* **117**(9) (2010) 1099–1109.

6. H. Adeli, S. Ghosh-Dastidar and N. Dadmehr, Alzheimer's disease and models of computation: Imaging, classification and neural models, *J. Alzheimer's Dis.* **7**(3) (2005) 187–199.

7. H. Adeli, S. Ghosh-Dastidar and N. Dadmehr, Alzheimer's disease: Models of computation and analysis of EEGs, *Clin. EEG Neurosci.* **36**(3) (2005) 131–140.

8. S. Ghosh-Dastidar, H. Adeli and N. Dadmehr, Voxel-based morphometry in Alzheimer's patients, *J. Alzheimer's Dis.* **10**(4) (2006) 445–447.

9. Z. Sankari, H. Adeli and A. Adeli, Wavelet coherence model for diagnosis of Alzheimer's disease, *Clin. EEG Neurosci.* **43**(3) (2012) 268–278.

10. Z. Sankari and H. Adeli, Probabilistic neural networks for EEG-based diagnosis of Alzheimer's disease using conventional and wavelet coherence, *J. Neurosci. Methods* **197**(1) (2011) 165–170.

11. S. Ghosh-Dastidar, H. Adeli and N. Dadmehr, Principal component analysis-enhanced cosine radial basis function neural network for robust epilepsy and seizure detection, *IEEE Trans. Biomed. Eng.* **55**(2) (2008) 512–518.

12. H. Adeli, Z. Zhou and N. Dadmehr, Analysis of EEG records in an epileptic patient using wavelet transform, *J. Neurosci. Methods* **123**(1) (2003) 69–87.

13. S. Ghosh-Dastidar and H. Adeli, A new supervised learning algorithm for multiple spiking neural networks with application in epilepsy and seizure detection, *Neural Netw.* **22** (2009) 1419–1431.

14. A. V. Medvedev, A. M. Murro and K. J. Meador, Abnormal interictal gamma activity may manifest a seizure onset zone in temporal lobe epilepsy, *Int. J. Neural Syst.* **21**(2) (2011) 103–114.

15. D. Sherman, N. Zhang, M. Anderson, S. Garg, M. J. Hinich, N. V. Thakor and M. A. Mirski, Detection of nonlinear interactions of EEG alpha waves in the brain by a new coherence measure and its application to epilepsy and anti-epileptic drug therapy, *Int. J. Neural Syst.* **21**(2) (2011) 115–126.

16. R. Acharya U, S. V. Sree and J. S. Suri, Automatic detection of epileptic EEG signals using higher order cumulant features, *Int. J. Neural Syst.* **21**(5) (2011) 403–414.

17. M. Ahmadlou, H. Adeli and A. Adeli, Fractality and a wavelet-chaos-neural network methodology for EEG-based diagnosis of autistic spectrum disorder, *J. Clin. Neurophysiol.* **27**(5) (2010) 328–333.

18. M. Ahmadlou, H. Adeli and A. Adeli, Fuzzy synchronization likelihood-wavelet methodology for diagnosis of autism spectrum disorder, *J. Neurosci. Methods* **211**(2) (2012) 203–209.

19. H. Adeli and S. Ghosh-Dastidar, *Automated EEG-based Diagnosis of Neurological Disorders-inventing the Future of Neurology* (CRC press, Florida USA, 2010).

20. F. Cong, A. H. Phan, Q. Zhao, T. Huttunen-Scott, J. Kaartinen, T. Ristaniemi, H. Lyytinen and A. Cichocki, Benefits of multi-domain feature of mismatch negativity extracted by nonnegative tensor factorization from EEG collected by low density array, *Int. J. Neural Syst.* **22**(6) (2012) 1250025.

21. R. Harrison, R. Birchall, D. Mann and W. Wang, Novel consensus approaches to the reliable ranking of features for seabed imagery classification, *Int. J. Neural Syst.* **22**(6) (2012) 1250026.

22. U. R. Acharya, S. V. Sree, A. P. C. Alvin and J. S. Suri, Application of nonlinear and wavelet based features for the automated identification of epileptic EEG signals, *Int. J. Neural Syst.* **22**(2) (2012) 1250002.

23. W. Y. Hsu, Continuous EEG signal analysis for asynchronous BCI application, *Int. J. Neural Syst.* **21**(4) (2011) 335–350.

24. U. R. Acharya, S. V. Sree, S. S. Chattopadhyay, W. Yu and A. P. C. Alvin, Application of recurrence quantification analysis for the automated identification of epileptic EEG signals, *Int. J. Neural Syst.* **21**(3) (2010) 199–211.

25. O. Faust, U. R. Acharya, L. C. Min and B. H. C. Sputh, Automatic identification of epileptic and background EEG signals using frequency domain parameters, *Int. J. Neural Syst.* **20**(2) (2010) 159–176.

26. G. Santhanam, S. I. Ryu, M. Y. Byron, A. Afshar and K. V. Shenoy, A high-performance brain-computer interface, *Nature*, **442** (2006) 195–198.

27. N. V. Manyakov, N. Chumerin and M. M. Van Hulle, Multichannel decoding for phase-coded SSVEP brain-computer interface, *Int. J. Neural Syst.* **22**(5) (2012) 1250022.

28. D. S. Tan and A. Nijholt, *Brain-computer Interfaces: Applying our Minds to Human-computer Interaction* (Springer-Verlag, London, 2010).

29. K. R. Muller, M. Krauledat, G. Dornhege, G. Curio and B. Blankertz, Machine learning techniques for brain-computer interfaces, *Biomed. Tech.* **49**(1) (2004) 11–22.

30. J. R. Wolpaw, D. J. McFarland, G. W. Neat and C. A. Forneris, An eeg-based brain-computer interface for cursor control, *Electroencephalogr. Clin. Neurophysiol.* **78**(3) (1991) 252–259.
31. D. J. McFarland, G. W. Neat, R. F. Read and J. R. Wolpaw, An eeg-based method for graded cursor control, *Psychobiology* **21**(1) (1993) 77–81.
32. D. J. McFarland, W. A. Sarnacki and J. R. Wolpaw, Electroencephalographic (EEG) control of three-dimensional movement, *J. Neural Eng.* **7**(3) (2010) 036007.
33. G. Schalk, D. J. McFarland, T. Hinterberger, N. Birbaumer and J. R. Wolpaw, BCI2000: A general purpose brain-computer interface (BCI) system, *IEEE Trans. Biomed. Eng.* **51**(6) (2004) 1034–1043.
34. G. Pfurtscheller, G. R. Muller, J. Pfurtscheller, H. J. Gerner and R. Rupp, Thought–control of functional electrical stimulation to restore hand grasp in a patient with tetraplegia, *Neurosci. Lett.* **351**(1) (2003) 33–36.
35. D. Huang, K. Qian, D. Y. Fei, W. Jia, X. Chen and O. Bai, Electroencephalography (EEG)-based brain-computer interface (BCI): A 2D virtual wheelchair control based on event-related desynchronization/synchronization and state control, *IEEE Trans. Neural Syst. Rehabil. Eng.* **20**(3) (2012) 379–388.
36. G. Pfurtscheller and C. Neuper, Future prospects of ERD/ERS in the context of brain-computer interface (BCI) developments, *Prog. Brain Res.* **159** (2006) 433–437.
37. R. Leeb, D. Friedman, G. R. Muller-Putz, R. Scherer, M. Slater and G. Pfurtscheller, Self-paced (asynchronous) BCI control of a wheelchair in virtual environments: A case study with a tetraplegic, *Comput. Intell. Neurosci.* **4** (2007) 1687–5265.
38. F. Galan, M. Nuttin, E. Lew, P. W. Ferrez, G. Vanacker, J. Philips and J. del R. Millan, A brain-actuated wheelchair: Asynchronous and non-invasive brain-computer interfaces for continuous control of robots, *Clin. Neurophysiol.* **119**(9) (2008) 2159–2169.
39. B. Rebsamen, E. Burdet, C. Guan, H. Zhang, C. L. Teo, Q. Zeng, M. Ang and C. Laugier, A brain-controlled wheelchair based on P300 and path guidance, *The First IEEE/RAS-EMBS Int. Conf. Biomedical Robotics and Biomechatronics* (BioRob 2006, 20–22, Feb. 2006), pp. 1101–1106.
40. B. Rebsamen, C. Guan, H. Zhang, C. Wang, C. Teo, M. H. Ang and E. Burdet, A brain controlled wheelchair to navigate in familiar environments, *IEEE Trans. Neural Syst. Rehabil. Eng.* **18**(6) (2010) 590–598.
41. C. S. Anthony and J. K. Zoltan, Principal-component localization of the source of the background EEG, *IEEE Trans. Biomed. Eng.* **42** (1995) 59–67.
42. H. Ramoser, G. J. Muller and G. Pfurtscheller, Optimal spatial filtering of single trial EEG during imagined hand movement, *IEEE Trans. Rehabil. Eng.* **8** (2000) 441–446.
43. V. Vapnik, *The Nature of Statistical Learning Theory* (Springer-Verlag, New York, 1995).
44. D. J. McFarland, L. M. McCane, S. V. David and J. R. Wolpaw, Spatial filter selection for EEG-based communication, *Electroencephalogr. Clin. Neurophysiol.* **103**(3) (1997) 386–394.
45. J. Li and L. Zhang, Active training paradigm for motor imagery BCI, *Exp. Brain Res.* **219**(2) (2012) 245–254.
46. K. Fukunaga, *Introduction to Statistical Pattern Recognition* (Academic Press, New York, 1972).